

Geiger-Mode Avalanche Photodiodes for Near-Infrared Photon Counting

Mark A. Itzler, Rafael Ben-Michael, Xudong Jiang, Krystyna Slomkowski

Princeton Lightwave Inc., 2555 US Route 130, Cranbury, New Jersey, 08512

E-mail: mitzler@princetonlightwave.com

Abstract: We present the design and characterization of InP-based avalanche photodiodes optimized for single photon counting for wavelengths between 1.0 and 1.7 μm , and we discuss performance trade-offs and mechanisms responsible for present performance limits.

©2007 Optical Society of America

OCIS codes: (040.5160) Photodetectors; (030.5260) Photon counting

To serve emerging applications at near-infrared (NIR) wavelengths between 1 and 1.7 μm , there has been a recent surge of interest in NIR photon counting detectors[1]. Dominant applications are found in the fields of communications and imaging, and single photon sensitivity is proving to be critical for sub-fields such as quantum cryptography and 3-D imaging. Photon counting at 1.5 μm is optimal for optical fiber-based technologies and also supports more eye-safe wavelengths ($>1.4 \mu\text{m}$) for imaging and ranging. Photon counting at 1.06 μm complements mature laser sources in applications such as lidar, ranging, and imaging when greater sensitivity is required.

Below its breakdown voltage V_b , an avalanche photodiode (APD) operates in linear mode, for which output photocurrent is proportional to input optical power. If an APD is biased above V_b , then a single photoexcited carrier can induce a run-away avalanche, giving rise to a detectable macroscopic current. Operating in this so-called Geiger mode, the detector is sensitive to a single photon and is referred to as a single photon avalanche diode (SPAD). In this paper, we describe our progress with SPAD design and performance and discuss mechanisms responsible for performance limitations through an analysis of activation energies found for dark count and afterpulse rates.

In Fig. 1, we present a schematic cross-section of our SPAD design platform[2]. The absorption layer consists of either InGaAs or InGaAsP lattice-matched to InP. InGaAsP absorbers provide much lower dark count rates in return for shorter cutoff wavelengths (suitable in, e.g., 1.06 μm applications). Avalanche gain is achieved in an undoped InP multiplication region of $\sim 1 \mu\text{m}$ thickness. To maintain high field in the multiplication region and low field in the absorption region, a moderately doped InP charge layer is placed between these regions. Since a heterointerface of InGaAs and InP tends to trap holes, a “grading” layer is employed to smooth this interface.

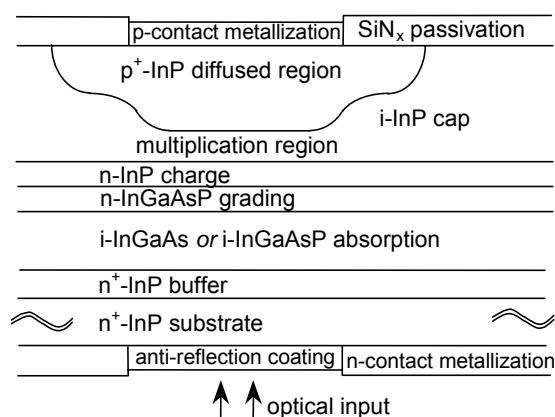


Fig. 1. Schematic cross-section of InP-based single photon avalanche diode (SPAD) structure.

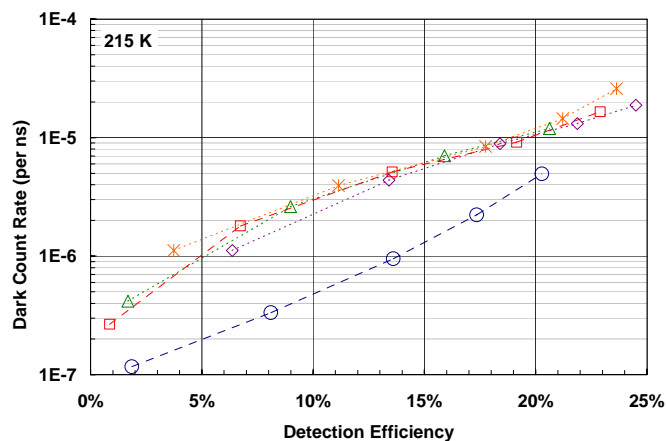


Fig. 2. Dark count rate vs. detection efficiency for $\phi 25 \mu\text{m}$ InGaAs/InP SPADs measured using 1 ns gating at 500 kHz, $T=215 \text{ K}$, and $\lambda=1.55 \mu\text{m}$.

The most fundamental performance characteristics of a SPAD are the probability of detecting an input photon, or the detection efficiency (DE), and the probability of measuring a false count when no photon is input, or the dark count rate (DCR). Both quantities increase with overbias voltage $V_{ov} \equiv V_{bias} - V_b$. For InGaAs/InP SPADs, V_{ov} is generally applied during a short time ($\sim 1 \text{ ns}$ to $\sim 100 \text{ ns}$) in gated mode operation. As seen in Fig. 2, for 25 μm diameter SPADs measured with 1 ns gates at 215 K, typical devices exhibit $\text{DCR} \sim 1 \times 10^{-5} \text{ ns}^{-1}$ at 20% DE, while occasional outliers (data indicated by “o”) show reduction by as much as $\sim 5\text{X}$ in DCR. Operation with 1 ns gates is desirable when photon arrival times are accurately known (e.g., in quantum communications). Higher DE can be achieved at the expense of higher DCR, and the optimal trade-off between DE and DCR is application-dependent.

A better understanding of the mechanisms behind dark carrier creation can be instrumental to reducing DCR. DCR vs. DE measurements at different temperatures show that DCR changes by a substantial factor ($\sim 1.5X - 2.5X$) for every 10K change in temperature. Temperature-dependent dark carrier creation mechanisms include generation-recombination via mid-gap states and thermally assisted tunneling via deep-level trap states in the absorption and multiplication regions. Plotting DCR vs. $1/(kT)$ to extract a DCR thermal activation energy $E_{a,DCR}$ lends insight into the thermal mechanisms involved. Often, this method is applied over a broad temperature range ΔT (e.g., $\Delta T > 50$ K), which assumes that the leakage mechanisms do not change over ΔT . In Fig. 3, we show $E_{a,DCR}$ obtained using exponential fits over much smaller temperature ranges (10 to 25 K). At temperatures below ~ 220 K, $E_{a,DCR}$ is small ($\sim 0.1 - 0.2$ eV), indicating the dominance of tunneling-related leakage mechanisms, and exhibits only a weak dependence on temperature. Above 220 K, $E_{a,DCR}$ increases rapidly, reaching $\sim 0.5 - 0.6$ eV by 270 K, indicating the dominance of thermal processes. For larger V_{ov} , tunneling mechanisms associated with lower $E_{a,DCR}$ persist until higher temperatures. The combination of experimental information such as that in Fig. 3 with detailed simulations following Ref. [3] provides considerable understanding of DCR behavior and aids further design optimization.

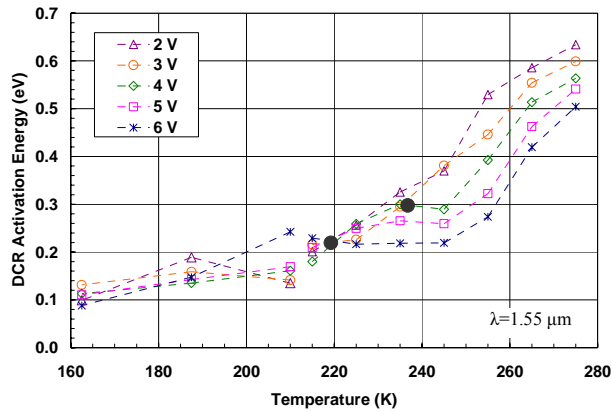


Fig. 3. DCR activation energy $E_{a,DCR}$ as a function of temperature at different overbiases (see legend). Data were obtained from three different set-ups: 1 ns gating (“•”), 20 ns gating (open symbols, $T \leq 210K$), and 100 ns gating (open symbols, $T \geq 220K$).

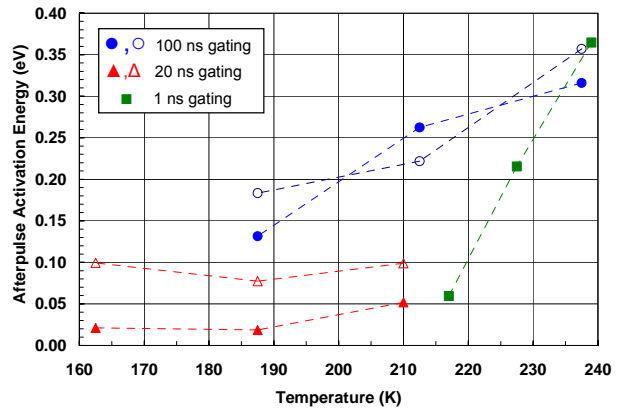


Fig. 4. Afterpulse activation energy $E_{a,AP}$ as a function of temperature obtained from five samples using three different measurement set-ups: 1 ns gating (squares), 20 ns gating (triangles), and 100 ns gating (circles).

Another important characteristic of SPAD performance is the trapping of avalanche-induced carriers at defects in the multiplication region and their subsequent release leading to additional dark counts. This phenomenon, referred to as afterpulsing, causes a dramatic increase in DCR when the time between gates (i.e., the inverse of the repetition rate) becomes small compared to the carrier detrapping time. Afterpulsing causes a serious performance tradeoff when high repetition rates are desired: afterpulsing effects can be reduced by operating at higher temperature, for which detrapping times decrease, but only at the expense of increased DCR.

Afterpulsing is determined by two fundamental parameters: the detrapping time for carrier release and the number of traps filled during avalanches. The number of traps filled will be dictated by the total number of traps and the amount of charge that flows during an avalanche event (roughly proportional to gate length). As for DCR, the determination of afterpulsing activation energies $E_{a,AP}$ provides insight into the nature of afterpulse mechanisms. In Fig. 4, we show $E_{a,AP}$ as a function of temperature (having neglected non-exponential temperature-dependent factors[4]) measured using different gate lengths for which charge flow occurs for widely varying durations (~ 1 ns, ~ 10 ns, and ~ 100 ns). Despite some quantitative differences, the trend towards larger $E_{a,AP}$ at higher temperature is consistent and suggests that thermal emission from traps is more prevalent as T increases from 200 K to 240 K.

In summary, we have described an InP-based SPAD structure that consistently provides dark count rates of $\leq 1 \times 10^{-5}$ per ns at 20% detection efficiency. Analysis of activation energies for DCR and afterpulsing shows that mechanisms responsible for these phenomena have significant variation over typical operating temperature ranges.

References

- [1] See Special Issue on “Single-Photon: Sources, Detectors, Applications, and Measurement Methods,” J. Modern Optics **54**, No. 2-3 (2007); see also Special Issue on “Single-Photon: Detectors, Applications, and Measurement Methods,” J. Modern Optics **51**, No. 9-10 (2004).
- [2] M.A. Itzler, R. Ben-Michael, C.-F. Hsu, K. Slomkowski, A. Tosi, S. Cova, F. Zappa, R. Ispasoiu, “Single photon avalanche diodes for 1.5 μ m photon counting applications,” J. Modern Optics **54**, No. 2-3, in press (2007).
- [3] J. P. Donnelly, E. K. Duerr, K. A. McIntosh, et al., “Design Considerations for 1.06- μ m InGaAsP-InP Geiger-Mode Avalanche Photodiodes,” IEEE J. Quantum Electron. **42**, 797-809 (2006).
- [4] K. E. Jensen, P. I. Hopman, E. K. Duerr, et al., “Afterpulsing in Geiger-mode avalanche photodiodes for 1.06 μ m wavelength,” Appl. Phys. Lett. **88**, 133503 (2006).